Energy Consumption Optimization for Mobile Robots in Three-dimension Motion Using Predictive Control

Mostafa I. Yacoub*, Dan S. Necsulescu**
Dept. of Mechanical Engineering
University of Ottawa
Ottawa, Canada
m_yacoub@aucegypt.edu

Jurek Z. Sasiadek**
Dept. of Mechanical & Aerospace Engineering
Carleton University
Ottawa, Canada
jurek_sasiadek@carleton.ca

***Abstract*—As the demand for field mobile robots in off-road operations increased, the need to investigate the 3D motion for mobile robots became important. One of the main difficulties in the 3D motion of a mobile robot is the torque saturation of the DC motors of the wheels that occurs while climbing hills. In the present work, off-road conditions are utilized to benefit by avoiding torque saturation. Energy optimization algorithm using predictive control is implemented on a two-DC motor-driven wheels mobile robot while crossing a ditch. The developed algorithm is simulated and compared with the PID control and the open-loop control. The predictive control showed more capability to avoid torque saturation and noticeable reduction in the energy consumption. Furthermore, using the wheels motors armature current instead of the supply voltage as control variable in the predictive control showed more robust speed control. Simulation results showed that in case of knowing the ditch dimensions ahead of time, the developed algorithm is feasible.**

Keywords—mobile robots; off-road conditions; predictive control; energy consumption; torque saturation

I. INTRODUCTION

Various proposals were published lately to reduce the energy consumption of electrically driven unmanned vehicles or the mobile robots.

Chuy *et al*. presented a model of power consumption of a skid-steered wheeled robotics ground vehicle [1]. The power model was used to determine combinations of linear velocity and turning radius of the robotic ground vehicle. Morales *et al*. adopted a kinematic approach to provide a simplified power consumption model and identification for wheeled skid-steer mobile robotic vehicles on hard horizontal ground [2]. The model estimates the motor power consumption as a function of the left- and right-side wheels' speeds. In 2010, Wei Yu *et al.* presented a dynamic model of a skid-steered wheeled vehicle for the general 2-D motion and the linear 3-D motion [3]. The models include motor saturation and power limitations. The authors carried out also experimental validation to the model. The main aim of the study was to provide velocity commands to the right and left wheels in case of open-loop and closed-loop control. They implemented a functional relationship between the terrain shear stress and shear displacement. The results showed good velocity accuracy with the PID controller over the open-loop control.

Zhang *et al.* introduced an approach to minimize the power consumption of a mobile robot by controlling its travelling speed and the frequency of its on-board processor simultaneously [4]. The problem is formulated as a discrete-time optimal control problem with a random terminal time and probabilistic state constrains. The simulation results show that the proposed method can save a significant amount of energy compared with some heuristic schemes. Suntharalingam *et al.* presented a gear locking mechanism to enhance acceleration and regenerative braking efficiency [5]. The simulation results show that this variable gear transmission achieve 33% higher acceleration performance compared with the fixed gear transmission ratio for the same power output motor. Similarly, the pure regenerative braking distance is reduced by 14%. Interestingly, Ngo *et al.* introduced a new concept, potentially distributable energy [6]. The proposed concept enables the mobile robots in a multi-robot field to partially recharge each other's batteries whenever they went low instead of going to the fixed mother charging station. The concept also assumes that not only the robots are capable of charging themselves, but also of exchanging batteries with each other. The concept aims to expand the autonomy of mobile robots by increasing their operating time without the human intervention. Spangelo and Egeland applied optimal-control method for trajectory planning and collision avoidance for underwater vehicles [7]. They suggested using piecewise linear parameterization with moderate number of parameters. Vanualailaiet *et al.* [8] introduced an asymptotically stable collision avoidance approach applied on a point mass using artificial potential fields with a solution to the local minima problem. The system is applied successfully to a nonholonomic planner mobile robot moving in the presence of a static obstacle.

Model Predictive Control (MPC) refers to a class of computer control algorithms that utilize an explicit process model to predict the future response of a plant [9]. At each control interval an MPC algorithm attempts to optimize future plant behavior by computing a sequence of future manipulated variable adjustments. The first step input in the optimal sequence is sent to the plant and the entire calculation is repeated at subsequent control intervals. Originally developed

978-1-4673-5769-2/13/$31.00 ©2013 IEEE

to meet the specialized control needs of power plant and petroleum refineries, MPC technology can now be found in a wide variety of applications including chemical, food processing, automotive, and aerospace applications [9], [10].

There are different types of MPC, but in the present work Dynamic Matrix Control (DMC) is considered due to its simplicity and effectiveness in the same time. In 1994, Berlin and Frank [11] presented a design and realization of a Multi-Input-Multi-Output (MIMO) predictive controller for a 3-tank system. They based their work on an extended DMC law. They showed how the predictive controllers can guarantee an excellent reference feedforward decoupling without the necessity of additional computation.

In the present work, an investigation of the control strategies of the electric drive motors of unmanned wheeled vehicles that serve in off-road environment is presented. The aim of the study is to develop a control strategy to improve the energy consumption of such a vehicle. An MPC controller is presented to optimize the energy consumption of such a mobile robot while moving downhill followed by moving uphill. The controller aims to take benefit from the kinetic energy gained during the downhill phase to minimize the consumed electric energy while going uphill. The DC motor performance is measured in case of using MPC controller and compared with that when using open-loop control as well as PID control. The simulation results were verified experimentally using the mobile robot shown in Fig.1. Experimental verification results will be presented in a subsequent paper.

The remainder of the paper is organized as follows: The second section includes a mathematical model of the mobile robot. The third section shows the simulation of the mobile robot with the three types of control: open-loop control, PID control, and the MPC control. In the fourth section, the simulation results are presented and discussed. Finally, the fifth section concludes the paper and includes recommendations for future work.

II. Mobile Robot Model

The mobile robot model implemented in the present work has two PM DC motor-driven wheels and a caster wheel. Through all the simulations, it is assumed that the robot is moving in a straight forward direction. The model of the PM DC motor is as follows [12]:

$$V_a - V_{brush} - R_a.I_a - K_a.\omega = L_a.dI_a/dt \quad (1)$$

$$I_a.K_a - \omega.D - T_{mech} = J.d\omega/dt \quad (2)$$

where,

V_a is the input DC voltage,
V_{brush} is the voltage drop in brushes,
R_a is the armature coil wire resistance,
I_a is the armature current,
K_a is the motor constant,
ω is the motor angular speed,
D is the damping coefficient,
L_a is the inductance of the motor coil,

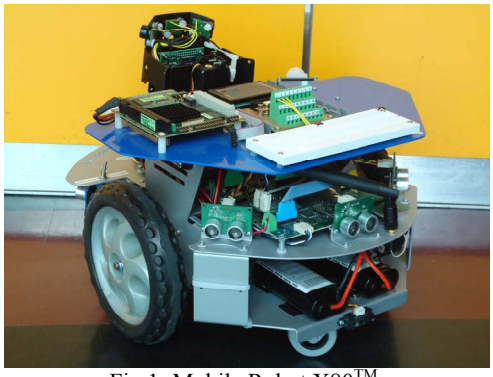

Fig.1: Mobile Robot X80™.

and J is the mass moment of inertia of the motor drive shaft and wheel assembly.

The mobile robot is assumed to move with relatively low speed and air resistance is neglected. The total resisting force due to car motion, ΣR, can be represented as follows [13]:

$$\Sigma R = \Theta ma + Gf\cos\alpha + G\sin\alpha \quad (3)$$

where,

G is the gross weight of the vehicle,
Θ is a dimensionless mass factor (usually with values of approx. 1.05 [13]) which includes the contribution of the of rotating wheels and other rotating masses in the car,
m is the total mass of the vehicle,
a is the acceleration of the vehicle,
f is the coefficient of rolling resistance between the wheel and the ground,
α is the angle of the slope of the road.

The total resisting load torque on each of the two motors due the car motion, T_{mech}, is

$$T_{mech} = \frac{G.r_d.i_{g.b}}{2\eta_m}\left[\frac{\Theta.r_d.i_{g.b}}{g}\frac{d\omega}{dt} + f\cos\alpha + \sin\alpha\right] \quad (4)$$

where,

r_d is the dynamic radius of the car wheel,
g is the gravitational acceleration,
$i_{g.b}$ is the reduction gearbox ratio,
η_m is the mechanical efficiency of the gearbox.

III. Simulation

All simulations are done using MATLAB™ SIMULINK™ for a total sampling time of 14s. The solver used is ode45 (Dormand-Prince) with a variable-step size and a relative tolerance of 10^{-3}. The robot is attempting to cross a 4.3 m wide ditch with: a 1.2 m level road, a 1.5 m downhill ramp, a 1.1 m uphill ramp, and a 0.5 m level road. The downhill slope angle of the ditch is -47° and the uphill angle is 13°. The parameters used in the simulation are those of the X80™ mobile robot [14].

A. Open-loop control

The open-loop control model is simulated using SIMULINK™ shown in Fig.2. The robot is subject to a

sudden input constant DC voltage and is allowed to attempt overcome the ditch.

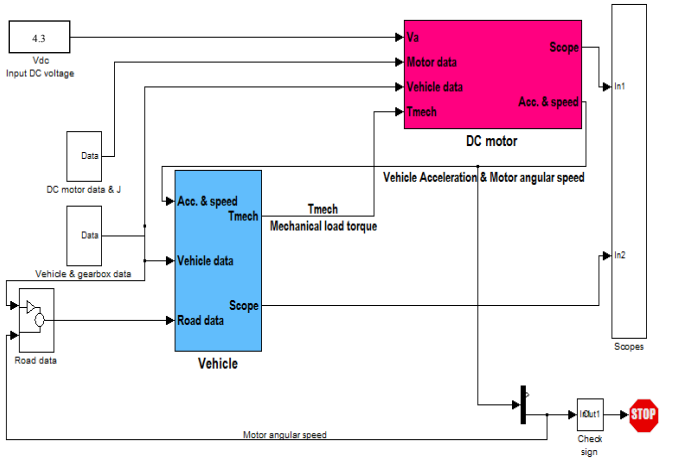

Fig.2: Open-loop control model layout of X80™ mobile robot.

B. PID speed control

The PID speed controller is applied to the robot using the speed feedback. The SIMULINK™ model is shown in Fig.3.The gains of the PID controller are K_P=10, K_I=0.7, and K_D=0.01.

C. Model Predictive Control (MPC)

The fact that all physical systems have constraints: physical constraints, e.g. actuators constraints; safety constraints, e.g. temperature/ pressure limits; and performance constraints, e.g. overshoot, and also the fact that optimal operating points are often near those constraints let the predictive control have a significant impact on the industrial control engineering. There is a noticeable expansion of the use of the predictive control in faster applications like automotive traction and engine control aerospace applications, and autonomous vehicles due to the significant improvement in the computation hardware.

The Dynamic Matrix Control (DMC), one of the MPC types, is considered here as it is the base of the MATLAB™ MPC toolbox [11], [15]. A discrete time state space description of n[th] order Multi-Input-Multi-Output (MIMO) system with r inputs and q outputs is considered

$$x_{k+1}=Ax_k+Bu_k$$
$$y_k=Cx_k \quad (5)$$

where,

x_{k+1} is the state vector at time $k+1$,
x_k is the state vector at time k ,
u_k is the input vector at time k ,
y_k is the output vector at time k ,
A, B, and C are the system discrete state space matrices.

The DMC could be applied by minimizing the quadratic cost function

$$J_k=\sum_{i=1}^{M} e_{k+i}^{T} Q_i e_{k+i}+\sum_{i=1}^{N} u_{k+i}^{T} R_i u_{k+1} \quad (6)$$

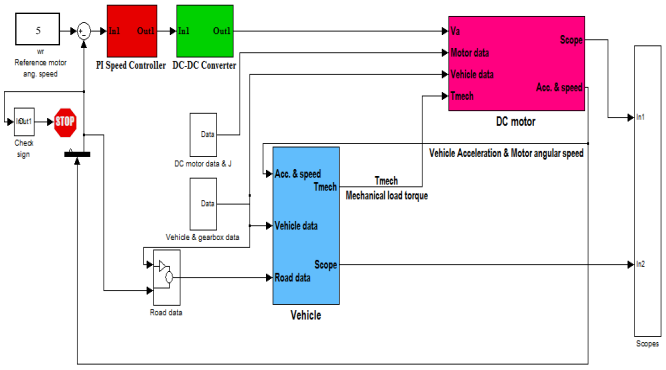

Fig.3: PID speed control model layout of the mobile robot.

where,

$e_{k+i}=w_{k+i}-y_{k+i}$ is future tracking error vector,
w_{k+i} is future reference trajectory vector,
y_{k+i} is future plant output vector,
u_{k+i} is future control signal vector,
Q_i, R_i are nonnegative diagonal weighting matrices,
M is optimization horizon,
and N is control horizon.

The $q\times q$ and $r\times r$ weighting matrices Q_i and R_i, respectively, can contain different weighting factors for each input and output. Using the state space description in equation (5) future values of the output vector, y, can be calculated as [11]

$$\underbrace{\begin{bmatrix} y_{k+1} \\ y_{k+2} \\ \vdots \\ y_{k+M} \end{bmatrix}}_{Y} = \underbrace{\begin{bmatrix} CA \\ CA^2 \\ \vdots \\ CA^M \end{bmatrix}}_{T} x_k + \underbrace{\begin{bmatrix} CB & 0 & \cdots & 0 \\ CAB & CB & & 0 \\ \vdots & \vdots & & \vdots \\ CA^{M-1}B & \cdots & CA^{M-N}B & 0 \end{bmatrix}}_{S} \underbrace{\begin{bmatrix} u_{k+1} \\ u_{k+2} \\ \vdots \\ u_{k+N} \end{bmatrix}}_{U} \quad (7)$$

Depending on the actual state vector, x_k, and the future control signals, u_{k+I}, the composite vector, Y, contains the future output vectors, while the matrix T describes the free motion of the MIMO system in equation (5). Equation (6) can be rewritten in matrix form as

$$J_k=(W-Y)^T \hat{Q}(W-Y)+U^T \hat{R}U \quad (8)$$

where the composite vector W contains the future reference vectors. The composite weighting matrices can be calculated as

$$\hat{Q}=diag(Q_1,Q_2,...,Q_M)$$
$$\hat{R}=diag(R_1,R_2,...,R_n) \quad (9)$$

The optimal composite control vector U can be obtained by minimizing the cost function with respect to U. Only the first vector u_k is going to be fed to the MIMO plant.

$$U = (\hat{R} + S^T \hat{Q} S)^{-1} S^T \hat{Q}(W - Tx_k) \quad (10)$$

The MPC is implemented here twice. First considering the armature DC voltage as a manipulated variable, and second considering the armature current as the manipulated variable.

1) MPC with DC voltage manipulated variable

The MATLAB™ MPC toolbox implicitly converts the continuous state space model into a discrete one, so it is only required here to derive the continuous state space mobile robot model. The state space model developed here includes the state vector as the motor angular speed, ω, and the armature current, I_a. The inputs to the system are the armature DC voltage supply, V_a, as a manipulated variable and the mechanical load torque, T_{mech}, as a measured disturbance. The supply voltage is chosen here as a control variable as it is a measure of the electric energy consumed by the DC motors. Another input is added here which is the voltage drop on the brushes, V_{brush}, but it is assumed to be a constant unmeasured disturbance. The outputs are assumed to be as the state vector and both states are assumed to be measurable. The continuous time state space model for the system is

$$\begin{bmatrix} \dot{x}_1 \\ \dot{x}_2 \end{bmatrix} = \begin{bmatrix} \dot{\omega} \\ \dot{I}_a \end{bmatrix} = \underbrace{\begin{bmatrix} \frac{-D}{J} & \frac{K_a}{J} \\ \frac{-K_a}{L_a} & \frac{-R_a}{L_a} \end{bmatrix}}_{A} \begin{bmatrix} \omega \\ I_a \end{bmatrix} + \underbrace{\begin{bmatrix} 0 & \frac{-1}{J} & 0 \\ \frac{1}{L_a} & 0 & \frac{-1}{L_a} \end{bmatrix}}_{B} \begin{bmatrix} V_a \\ T_{mech} \\ V_{brush} \end{bmatrix} \quad (11)$$

$$\begin{bmatrix} y \end{bmatrix} = \underbrace{\begin{bmatrix} 1 & 0 \\ 0 & 1 \end{bmatrix}}_{C} \begin{bmatrix} \omega \\ I_a \end{bmatrix} + \underbrace{\begin{bmatrix} 0 & 0 & 0 \\ 0 & 0 & 0 \end{bmatrix}}_{D} \begin{bmatrix} V_a \\ T_{mech} \\ V_{brush} \end{bmatrix} \quad (12)$$

The MPC controller design uses here a prediction horizon of 400 time steps, a control horizon of 400 time steps, and a sample time of 0.02 s. Also, an optimization weighting factor of unity is assumed for the DC voltage supply and 0.1 for both the speed and armature current error minimization. Those weighting factors were obtained using trial and error. The constraints for the voltage (which is a measure of the electric energy as mentioned earlier) and the speed are

$$-4.3 \le V_a \le 4.3V \quad (13)$$

$$\omega > 0 \quad (14)$$

The block diagram of the MPC control using the voltage as a manipulated variable is shown in Fig.4.

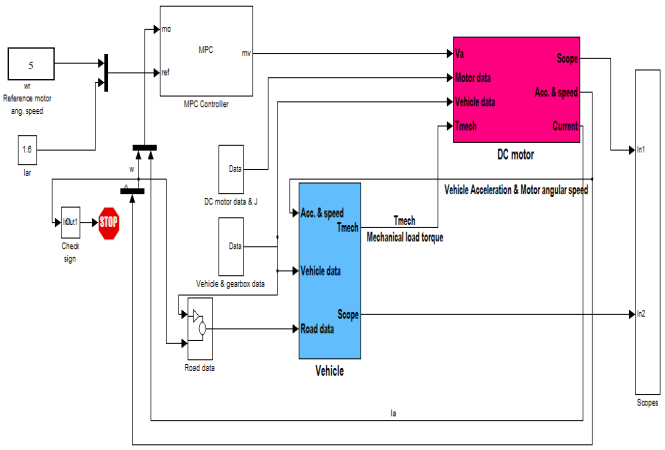

Fig.4: Layout of mobile robot MPC control using the voltage as a manipulated variable.

2) MPC with DC current manipulated variable

Since the continuous state space model is required here too, a new variable, S_a, is introduced

$$S_a = \int V_a(t)dt \quad (15)$$

so that equation (1) and (2) could be rewritten as

$$\frac{dS_a}{dt} = V_a = \frac{1}{0.98}\left[L_a \frac{dI_a}{dt} + R_a I_a + K_a \omega\right] \quad (16)$$

$$\frac{d\omega}{dt} = \frac{1}{J}\left[I_a K_a - \omega D - T_{mech}\right] \quad (17)$$

where the multiplier factor in equation (16) arises from the assumption that the voltage drop in the brushes is 2% of the input voltage for simplicity.

Now the state variables are the integration of the armature voltage, S_a, and the motor speed, ω. The inputs are the current, I_a, and the mechanical load torque, T_{mech}. The outputs are the same as the state variable. The continuous time state space representation of the system is

$$\begin{bmatrix} \dot{x}_1 \\ \dot{x}_2 \end{bmatrix} = \underbrace{\begin{bmatrix} \frac{dS_a}{dt} \\ \frac{d\omega}{dt} \end{bmatrix}}_{\dot{x}} = \underbrace{\begin{bmatrix} 0 & \frac{K_a}{0.98} \\ 0 & \frac{-D}{J} \end{bmatrix}}_{A} \underbrace{\begin{bmatrix} S_a \\ \omega \end{bmatrix}}_{x} + \underbrace{\begin{bmatrix} \frac{R_a}{0.98} & 0 \\ \frac{K_a}{J} & \frac{-1}{J} \end{bmatrix}}_{B_1} \underbrace{\begin{bmatrix} I_a \\ T_{mech} \end{bmatrix}}_{u} + \underbrace{\begin{bmatrix} \frac{L_a}{0.98} & 0 \\ 0 & 0 \end{bmatrix}}_{B_2} \underbrace{\begin{bmatrix} \dot{I}_a \\ \dot{T}_{mech} \end{bmatrix}}_{\dot{u}} \quad (18)$$

$$\begin{bmatrix} y \end{bmatrix} = \underbrace{\begin{bmatrix} 1 & 0 \\ 0 & 1 \end{bmatrix}}_{C} \underbrace{\begin{bmatrix} S_a \\ \omega \end{bmatrix}}_{x} + \underbrace{\begin{bmatrix} 0 & 0 \\ 0 & 0 \end{bmatrix}}_{D} \underbrace{\begin{bmatrix} I_a \\ T_{mech} \end{bmatrix}}_{u} \quad (19)$$

The fact that the MATLAB™ MPC toolbox doesn't accept a derivative input, brings a need to reform the state space representation using Porter & Bradshaw approach [16]. A new state space representation is constructed as follows

$$\dot{X}_1(t) = AX_1(t) + BU_1(t) \quad (20)$$

$$Y_1(t) = X_1(t) + B_2 U_1(t) \quad (21)$$

where $$B = B_1 + AB_2 \quad (22)$$

$$\begin{bmatrix} X_1(t) \\ U_1(t) \end{bmatrix} = \begin{bmatrix} I_n & -B_2 \\ O_{l,n} & I_l \end{bmatrix} \begin{bmatrix} x(t) \\ u(t) \end{bmatrix} \quad (23)$$

where n is the number of the original states and l is the number of the original inputs, I_n is the identity matrix of dimension n and I_l is the identity matrix of dimension l, and finally $O_{l,n}$ is zero matrix of dimension $l \times n$.

Applying this approach to the present system gives the new continuous time state space representation as follows:

$$\dot{X}_1(t) = \underbrace{\begin{bmatrix} 0 & \frac{K_a}{0.98} \\ 0 & \frac{-D}{J} \end{bmatrix}}_{A} \underbrace{\begin{bmatrix} S_a - \frac{L_a \dot{I}_a}{0.98} \\ \omega \end{bmatrix}}_{X_1(t)} + \underbrace{\begin{bmatrix} \frac{R_a}{0.98} & 0 \\ \frac{K_a}{J} & \frac{-1}{J} \end{bmatrix}}_{B} \underbrace{\begin{bmatrix} I_a \\ T_{mech} \end{bmatrix}}_{U_1(t)} \quad (24)$$

$$Y_1(t) = \underbrace{\begin{bmatrix} 1 & 0 \\ 0 & 1 \end{bmatrix}}_{C} X_1(t) + \underbrace{\begin{bmatrix} 0 & 0 \\ 0 & 0 \end{bmatrix}}_{D} U_1(t) \quad (25)$$

The four new obtained matrices, *A*, *B*, *C*, and *D*, are used in the MPC toolbox.

IV. Simulation Results

In this section, the simulation results will be presented and a comparison of the mobile robot DC motors performance for different kinds of control will be discussed. Throughout this section, the performance of a DC motor is going to be presented by ten graphs illustrating ten parameters in each figure case. The first two graphs in each figure are road slope *α(t)* (left) and DC input voltage (right). The second two graphs are the mechanical load torque T_{mech} (left) and armature current, I_a(right). The third two graphs are the robot wheel angular speed (left) and the electric input power fed to the motor $P_{in} = I_a.V_a$ (right). The fourth two graphs are the mechanical delivered power to the wheels $P_{out} = T_{mech}.\omega$ (left) and the induced e.m.f. E_a (right). The fifth two graphs are the mobile robot normalized acceleration, $\xi = (1/g).(dv/dt)$ (left) and the motor electromagnetic torque, T_{em}, (right).

A. Open-loop control results

Fig.5 shows the simulation results obtained when using open-loop control and constant DC voltage input.

The results indicate that the robot failed to cross the ditch (it succeeds to go downhill but fails to reach the top of the hill). This is shown in the road grade graph where the robot stayed at the uphill portion trying to overcome it. That's what's called the torque saturation.

B. PID control results

Simulation results when using PID speed control by controlling the DC supply voltage are shown in Fig. 6. The results indicated good speed control but high power and energy consumption (7 W and 45 J respectively during the entire operation).

C. MPC control results

Fig.7 shows the simulation results of the MPC control when using the DC voltage as a manipulated variable.

The results indicate a noticeable improvement in the power and energy consumption (3 W and 16.5 J respectively).

The simulation results of the DC motor performance when controlled by MPC control using the armature current as a manipulated variable are shown in Fig.8. The results indicate that there is also an improvement in the power and energy consumption (in average 2.7 W and 21 J respectively) but, in

Experimental setup was built to validate the simulation results. The description of the test rig is as follows:

- Wood made ramps are used to reproduce the ditch with the dimensions used in the simulation.
- X80 Dr. Robot™ mobile robot is used which has the same parameters used in the simulation as mentioned earlier, Fig.1.
- The voltage profiles obtained from the simulations are fed to the DC motors as inputs.
- The DC supply voltage, the armature current, the motor angular speed and the distance covered are measured during the experiments.
- The experiments are implemented for open-loop control, PID control and MPC control.

Comparing the experimental results with those obtained from the simulation, a good agreement between them could be noticed as it will be illustrated in a subsequent paper.

In general, the MPC control gives noticeable economy of power and energy consumption in both cases, when using the DC voltage as a manipulated variable and when using the

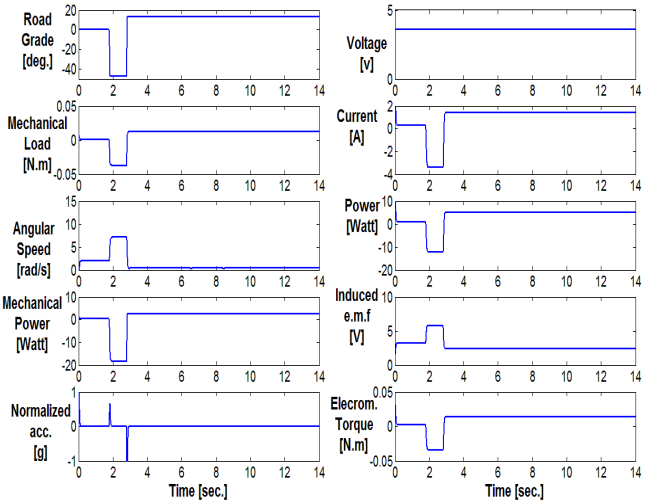

Fig.5: DC motor performance using open-loop control with constant input DC voltage.

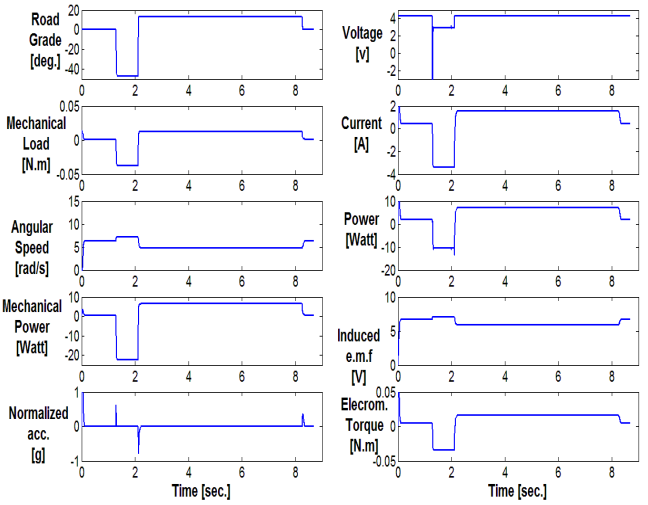

Fig. 6: DC motor performance using PID speed control by controlling the DC supply voltage.

armature current as a manipulated variable. Furthermore, when using the current as a manipulated variable in MPC speed control, a more robust speed control is achieved.

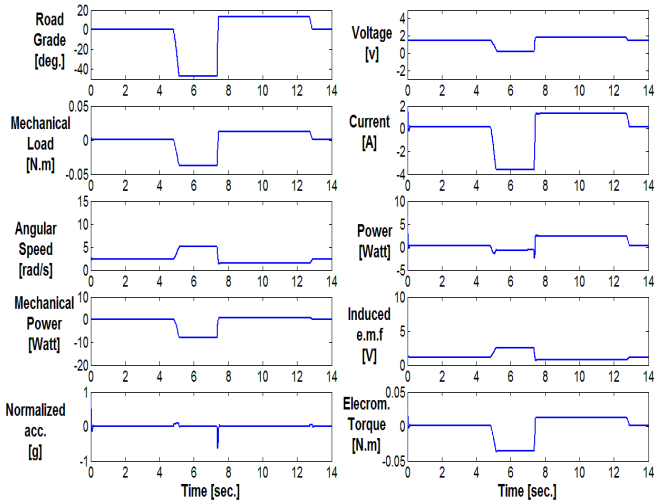

Fig.7: DC motor performance with MPC control using the DC voltage as a manipulated variable.

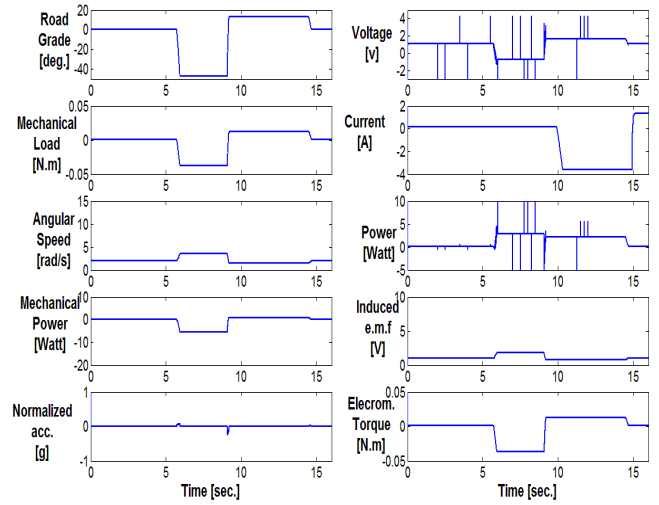

Fig.8: DC motor performance with MPC control using the armature current as a manipulated variable.

V. CONCLUSIONS

A solution to the torque saturation problem of mobile robots wheels drives is presented and applied to a developed model of a mobile robot. Energy optimization using predictive control is applied to the developed mobile robot model attempting to overcome a ditch. Given the 3D map ahead of time, the simulation results showed how the predictive control was able to avoid torque saturation unlike the open-loop control. In addition, the predictive control succeeded to economize energy consumption compared with the PID control. Furthermore, using the armature current instead of the supply voltage as control variable showed more robust speed control as well as reduced energy consumption. The results encourage investigating different 3D map features in future like irregular holes and hills.

It is recommended for future work to implement a parametric study to address the effects of different parameters on the energy consumption. Finally, a practical method to detect dimensions of the obstacle ahead of time needs to be investigated.

REFERENCES

[1] O. Chuy, E. Collins, W. Yu, and C. Ordonez, "Power modeling of a skid steered robotic ground vehicle," in *IEEE International Conference on Robotics and Automation*, Kobe, 2009.

[2] Jesus Morales, Jorge L. Martinez, Antjony Mandow, Alejandro Pequeno-Boter, and Alfonso Garcia-Cerezo, "Simplified power consumption modeling and identification for wheeled skid-steer robotic vehicles on hard horizontal ground," in *IEEE/RJ International Conference on Intelligent Robots and Systems*, Taiwan, 2010.

[3] Wei Yu, Oscar Ylaya Chuy, Emmanuel G. Collins, and Partick Hollis, "Analysis and experimental verification for dynamic modeling of a skid-steered wheeled vehicle," *IEEE Transactions on Robotics*, vol. 26, no. 2, April 2010.

[4] W. Zhang, Y. Lu, and J. Hu, "Optimal solutions to a class of power management problems in Mobile Robots," *Automatica (Journal of IFAC)*, vol. 45, no. 4, pp. 989-996, April 2009.

[5] P. Suntharalingam, J. T. Economou, and K. Knowles, "Gear locking mechanism to extend the consistent power operating region of the electric motor to enhance acceleration and regenerative braking efficiency in hybrid electric vehicles," in *IEEE Vehicle Power and Propulsion Conference*, Dearborn, MI, 2009.

[6] Trung Dung Ngo, Hector Raposo, and Henrik Schioler, "Potentially distributable energy: Towards energy autonomy in large population of mobile robots," in *Proceedings of the 2007 IEEE International Symposium on Computational Intelligance in Robotics and Automation*, Jacksonville, FL, 2007.

[7] Inge Spangelo and Olav Egeland, "Trajectory planning and collision avoidance for underwater vehicles using optimal control," *IEEE Journal of Oceanic Engineering*, vol. 19, no. 4, October 1994.

[8] Jito Vanualailai, Bibhya Sharma, and Shin-ichi Nakagiri, "An asymptotically stable collision-avoidance system," *International Journal of Nonlinear Mechanics*, vol. 43, no. 9, pp. 925-932, November 2008.

[9] S. Joe Qin and Thomas A. Badgwell, "A survey of industrial model predictive control technology," *Control Engineering Practice (Journal of IFAC)*, vol. 11, pp. 733-764, 2003.

[10] J. B. Rawlings, "Tutorial overview of model predictive control," *IEEE Cotrol Systems Magazine*, vol. 20, no. 3, pp. 38-52, June 2000.

[11] F. Berlin and P. M. Frank, "Design and realization of a MIMO predictive controller for a 3-tank system," *Advances in Model-Based Predictive Control, Oxford University Press*, pp. 446-457, 1994.

[12] Chee-Mun Ong, "DC machines," in *Dynamic simulations of electric machinery: Using MATLAB/SIMULINK*. New Jersey: Prentice Hall, 2006, ch. 8, pp. 351-401.

[13] Jo Yung Wong, "Performance characteristics of road vehicles," in *Theory of Ground Vehicles*. New York: John Wiley & Sons Inc., 2001, ch. 3, pp. 203-294.

[14] Dr Robot Inc. (2012, May) X80: An industrial grade robot for research and development applications. [Online]. http://www.drrobot.com/products/item_downloads/x80_1.pdf

[15] MathWorks Inc. (2011, September) Model predictive control toolbox user's guide. [Online]. http://www.mathworks.com/help/pdf_doc/mpc/mpc_ug.pdf

[16] B. Porter and A. Bradshaw, "Multivariable time-invariant linear systems with input-derivative control: state controllability and eigenvalue assignability," *International Journal of Control*, vol. 16, no. 1, pp. 101-104, 1972.